E6 and E7 Gene Silencing and Transformed Phenotype of Human Papillomavirus 16–Positive Oropharyngeal Cancer Cells

Theodore Rampias, Clarence Sasaki, Paul Weinberger, Amanda Psyrri

Background The *E6* and *E7* genes of human papillomavirus type 16 (HPV16) encode oncoproteins that bind and degrade p53 and retinoblastoma (pRb) tumor suppressors, respectively. We examined the effects of repressing *E6* and *E7* oncogene expression on the transformed phenotype of HPV16-positive oropharyngeal cancer cell lines.

Methods Human oropharyngeal squamous cell cancer 147T and 090 (harboring integrated HPV16 DNA) and 040T (HPV DNA–negative) cells were infected with retroviruses that expressed a short hairpin RNA (shRNA) targeting the HPV16 *E6* and *E7* genes or a scrambled-sequence control shRNA. Flow cytometry, terminal deoxynucleotidyltransferase–mediated UTP end-labeling assay, and immunoblotting for annexin V were used to assess apoptosis in shRNA-infected cell lines. Biochemical analysis involved quantitative real-time polymerase chain reaction analysis of p53- and pRb-target gene expression and immunoblotting for p53 and pRb protein expression.

Results In 147T and 090 cells, shRNA-mediated inhibition of HPV16 *E6* and *E7* expression reduced the *E6* and *E7* mRNA levels by more than 85% compared with control cells that expressed a scrambled-sequence shRNA. *E6* and *E7* repression resulted in restoration of p53 and pRB protein expression, increased expression of p53-target genes (*p21* and *FAS*), decreased expression of genes whose expression is increased in the absence of functional pRb (*DEK* and *B-MYB*), and induced substantial apoptosis in 147T and 090 cells compared with the control shRNA–infected cells (from 13.4% in uninfected to 84.3% in infected 147T cells and from 3.3% in uninfected to 71.2% in infected 090 cells).

Conclusion Repression of *E6* and *E7* oncogenes results in restoration of p53 and pRb suppressor pathways and induced apoptosis in HPV16-positive oropharyngeal squamous cell cancer cell lines.

J Natl Cancer Inst 2009;101:412–423

Almost all cases of cervical carcinoma are initiated by infection with high-risk human papillomaviruses (HPVs) (1). Numerous lines of epidemiological and molecular pathology evidence also suggest that some of the high-risk HPVs, especially HPV type 16 (HPV16), are etiologically related to a subset of head and neck squamous cell carcinomas (2–6), in particular, those arising from the tonsils in individuals with no history of alcohol or tobacco use (4). In addition, from 1973 to 2001, the incidence of oropharyngeal cancer increased among white men and women aged 20–44 years, which paralleled an increase in the incidence of sexual practices associated with transmission of HPV16 (7–12). According to a workshop hosted by The Cancer Etiology Branch of the National Cancer Institute entitled "Validation of a Causal Relationship: Criteria to Establish Etiology" (13), four types of evidence are needed to establish a causal association in cancer: epidemiological, molecular pathological, experimental, and evidence derived from animal studies. There is substantial epidemiological and molecular pathology evidence indicating that HPV16 is associated with a subset of oropharyngeal cancers (2–6). However, experimental evidence showing that HPV16 is causally associated with a subset of oropharyngeal squamous cell carcinomas is lacking. Specifically, experimental data showing that transcriptionally active HPV16 is required for malignant transformation of HPV16-positive oropharyngeal cancer cells are needed to further support a causal association between HPV16 and a subset of oropharyngeal squamous cell carcinomas.

Studies in cervical cancer, the most widely acknowledged HPV-associated malignancy, indicate that HPV-driven malignant

Affiliations of authors: Department of Medical Oncology (TR, PW, AP) and Department of Otolaryngology (CS, PW), Yale University School of Medicine, New Haven, CT.

Correspondence to: Amanda Psyrri, MD, PhD, Yale University School of Medicine, New Haven, CT 06520 (dp237@email.med.yale.edu or psyrri237@yahoo.com).

See "Funding" and "Notes" following "References."

DOI: 10.1093/jnci/djp017

conversion is associated with the specific molecular events. For example, integration of viral DNA into the genome of the infected host cell often disrupts the viral gene that encodes the E2 protein, which is a transcription factor that can repress expression of the HPV *E6* and *E7* oncogenes (14–16). The *E6* and *E7* oncoproteins encoded by the high-risk HPVs bind and degrade the host p53 and retinoblastoma (pRb) tumor suppressor proteins, respectively (17,18). In vitro studies have shown that pRb and the pRb family members p107 and p130 regulate the activity of host-encoded E2F transcription factors and that complexes consisting of E2F and hypophosphorylated pRb repress the transcription of genes such as cyclin A that are required for cell cycle progression (19,20). The E7 protein encoded by high-risk HPVs binds to pRb family members and disrupts their ability to form complexes with E2F, resulting in increased expression of E2F-responsive genes, many of which are required for cell cycle progression (18–20). In addition, the E7 protein accelerates degradation of hypophosphorylated pRb family members (15). Most cervical carcinomas harbor wild-type *TP53* and *Rb* tumor suppressor genes. Thus, the tumor suppressor pathways in HPV-infected or -positive cervical carcinoma cells are intact but dormant due to the continuous expression of *E6* and *E7* genes.

There are strong experimental data showing that continued expression of the *E6* and *E7* oncogenes of high-risk HPVs is required for the maintenance of the proliferative state of cervical cancer cells. Several approaches to repress expression of *E6* and *E7*, such as antisense RNA strategies and expression of the bovine papillomavirus (BPV) *E2* gene, have been tested in human cervical carcinoma cell lines (14,21,22). *E2* gene–mediated *E6* and *E7* gene repression resulted in activation of the p53 and pRb pathways, inhibition of telomerase activity, and cellular growth arrest and senescence (14,23–25), whereas antisense RNA strategies led to a several-fold inhibition of cell proliferation (21,22). The effects of repression of HPV16 *E6* and *E7* oncogenes on the transformed phenotype of oropharyngeal squamous carcinoma cells have not been clearly demonstrated. In this study, we used retrovirus-mediated delivery of short hairpin RNAs (shRNAs) targeting HPV16 *E6* and *E7* in HPV16-positive and HPV16-negative oropharyngeal cancer cell lines to examine the effect of decreased *E6* and *E7* oncogene expression on cell survival and the p53 and Rb tumor suppressor pathways in human oropharyngeal cancer cell lines.

CONTEXT AND CAVEATS

Prior knowledge

Epidemiological and molecular pathology data have suggested that human papillomavirus type 16 (HPV16) is associated with a subset of oropharyngeal cancers, but experimental data showing a causal association between transcriptionally active HPV16 and HPV16-positive oropharyngeal squamous cell carcinomas are lacking.

Study design

Retrovirus-mediated delivery of short hairpin RNAs (shRNAs) targeting the HPV16 *E6* and *E7* oncogenes was used to examine the effect of decreased *E6* and *E7* oncogene expression on cell survival and the p53 and Rb tumor suppressor pathways in HPV16-positive and HPV16-negative human oropharyngeal cancer cell lines.

Contribution

shRNA-mediated repression of HPV16 *E6* and *E7* oncogene expression resulted in the activation of the p53 and pRb tumor suppressor pathways and in the induction of apoptosis in HPV16-positive oropharyngeal cancer cell lines.

Implications

Continuous expression of HPV *E6* and *E7* is required to maintain the proliferative state and to prevent apoptosis in HPV16-positive human oropharyngeal cancer cells.

Limitations

The study was limited to in vitro experimental data. Experimental evidence in an animal model will ultimately be needed to prove a causal association.

From the Editors

Materials and Methods

Cell Lines and Culture Conditions

The human cervical carcinoma cell lines HeLa (HPV18 positive) and SiHa (HPV16 positive) and human embryonic kidney 293T cells were obtained from the American Type Culture Collection (Manassas, VA). The human oropharyngeal squamous cell cancer cell lines 147T and 040T were a kind gift from Dr Renske Steenbergen (VU University Medical Center, Molecular Pathology Unit, Amsterdam, the Netherlands) (26), and the human oropharyngeal squamous cell cancer cell line 090 was a kind gift from Dr Susanne Gollin (University of Pittsburgh School of Public Health, Pittsburgh, PA) (27). The 147T cells stably express the HPV16 *E6* and *E7* transcripts and contain one to two integrated copies of HPV16 DNA per cell genome; the 040T cells lack detectable levels of HPV DNA (26). The 090 cells contain several integrated copies of transcriptionally active HPV16 DNA (27). All cell lines were maintained in Dulbecco's modified Eagle medium containing 10% fetal bovine serum (GIBCO Life Technologies Inc, Gaithersburg, MD) in a humidified (37°C, 5% CO_2) incubator, grown in 75-cm^2 culture flasks, and passaged when they reached 80% confluence.

shRNA Oligonucleotides and Retrovirus Production

All shRNA sequences targeting the HPV16 *E6* and *E7* transcripts were designed according to published criteria (28) by using the BLOCK-iT RNAi Designer algorithm (Invitrogen, Carlsbad, CA) and were screened against the human genome by using a BLAST search to assess sequence specificity and avoid unintentional silencing of host cell genes. We selected five different target sites within the bicistronically transcribed HPV16 *E6* and *E7* mRNAs according to the Invitrogen Web-based guidelines (https://rnaidesigner.classic.invitrogen.com/rnaiexpress/index.jsp) (Table 1). Complementary oligonucleotides encoding shRNAs that targeted each of these five sites were synthesized, annealed, and cloned into the pSIREN-RetroQ retroviral expression vector (BD Biosciences, San Jose, CA) at a site 3′ to the human U6 promoter, resulting in retroviral (RV) plasmids RV-shRNAHN1, RV-shRNAHN2, RV-shRNAHN3, RV-shRNAHN4, and RV-shRNAHN5. For a negative control shRNA, we cloned a scrambled-sequence oligonucleotide (5′-CTTACAATCAGACTGGCGA-3′) that could not form a hairpin into pSIREN-RetroQ, resulting in RV-control shRNA. The resulting

Table 1. Human HPV16 *E6* and *E7*-target sequences for shRNA oligonucleotides*

shRNA oligonucleotide	Nucleotide position in full-length *E6* and *E7* transcript†	Target sequence (5′ to 3′)
shRNAHN1	272–292	GGGAATCCATATGCTGTATGT
shRNAHN2	503–523	GGTCGATGTATGTCTTGTTGC
shRNAHN3	189–209	AATGTGTGTACTGCAAGCAAC
shRNAHN4	702–722	GGACAGAGCCCATTACAATAT
shRNAHN5	709–729	GCCCATTACAATATTGTAACC

* Five different shRNAs directed against human HPV16 *E6* and *E7* mRNA sequence were designed to correspond to different regions of transcript. Target sequences of shRNA oligonucleotides and corresponding positions in HPV16 *E6* and *E7* transcript are shown. HPV16 = human papillomavirus type 16; shRNA = short hairpin RNA; shRNAHN1 = shRNA oligo HN1; shRNAHN2 = shRNA oligo HN2; shRNAHN3 = shRNA oligo HN3; shRNAHN4 = shRNA oligo HN3; and shRNAHN5 = shRNA oligo HN5.

† Numbering according to Seedorf et al. (29).

plasmids were purified by using a HiSpeed Plasmid Maxi kit (Qiagen, Valencia, CA) according to the manufacturer's instructions, and the presence of the correct inserts was confirmed by DNA sequencing.

Retrovirus production and titration were performed as described previously (30). Briefly, to generate recombinant retroviruses that expressed the various shRNAs, 2×10^6 293T cells were plated on 100-mm plates and incubated overnight. The following day, subconfluent 293T cells (50%–60% confluency) were cotransfected by using the calcium phosphate precipitation method with 10 μg of pSIREN-RetroQ shRNA expression vector, 6 μg of packaging plasmid pCL-ECO (IMGENEX, San Diego, CA), and 4 μg of envelop vector pVSVg (Clonotech, Mountain View, CA), a helper plasmid expressing the vesicular stomatitis virus glycoprotein (VSV-G). After 8 hours, the medium was changed and substituted with OptiMEM (Invitrogen). The virus-containing supernatants were then harvested each day for 5 days, passed through 0.45-μm (pore size) membrane filters (Millipore MCE/MF, Billerica, MA), and concentrated by centrifugation with the use of Centricon Plus-20 filter devices (Fischer Scientific, Pittsburgh, PA) to generate viral stocks to be used for infection of oropharyngeal cell lines. The viral stocks were separated into aliquots and stored at −80°C. To determine the viral titer, the concentrated viral stocks were diluted 1:10 in RIPA buffer (25 mM Tris–HCl [pH 7.6], 150 mM NaCl, 1% NP-40, 1% sodium deoxycholate, and 0.1% sodium dodecyl sulfate [SDS]), incubated on ice for 15 minutes, and resolved by electrophoresis on a 12% SDS–polyacrylamide gel. The resolved viral proteins were transferred to an Immun-Blot polyvinylidene difluoride (PVDF) membrane (Bio-Rad Laboratories, Hercules, CA), and the membrane was incubated with a rabbit polyclonal antibody against VSV-G envelop protein (at 1:1500 dilution; Sigma-Aldrich, St Louis, MO). Antibody binding was detected with the use of an enhanced chemiluminescence kit (Amersham Biosciences, Freiburg, Germany). The viral titers from different concentrated viral stocks were compared by the intensity of the immunoreaction signal in immunoblot analysis. The volumes of viral stocks used for infection were adjusted by adding Dulbecco's modified Eagle medium containing 10% fetal bovine serum so that the viral loads would be equal. For infection, human oropharyngeal 140T, 040T, and 090 cells and cervical SiHa cells grown to approximately 60% confluency in 100-mm plates were incubated for 8 hours with 1 mL of the viral stocks in the presence of polybrene (Sigma-Aldrich) at 5 μg/mL. The medium was then replaced with fresh growth medium, and the infected cells were cultured for 5 days.

To confirm efficient transfection and integration of retroviral DNA into the genomes of the infected cells (140T, 040T, 090, and SiHa), we used a real-time polymerase chain reaction (PCR) assay to amplify the integrated retroviral DNA from the genomic DNA isolated from retrovirus-infected oropharyngeal and cervical cancer cell lines. This assay used cells infected with concentrated retrovirus expressing shRNAHN4, the oligonucleotide that exhibited the highest silencing efficiency. Briefly, 040T, 147T, 090, and SiHa cells were infected for 24 hours with concentrated retrovirus expressing shRNAHN4. Two days after infection, genomic DNA was isolated by using the QIAamp DNA Mini Kit (QIAGEN SA). Integrated DNA from the shRNAHN4-expressing virus was amplified by using a primer that anneals within the pSIREN-RetroQ shRNA expression plasmid sequence (GIAF: 5′-AGGGCCTATTTCCCATGAT-3′) and a specific primer complementary to shRNAHN4 oligo (SR: 5′-TAATGGGCTCTGTCCGGATC-3′). The primers actin1 (5′-TCCTGTGGCATCCACGAAACT-3′) and actin2 (5′-GAAGCATTTGCGGTGGACGAT-3′) were used to amplify the β-actin gene as the internal reference gene in separate reactions. As negative controls, we used samples of genomic DNA from uninfected cell lines. The genomic template (100 ng) was amplified in a volume of 25 μL that contained the qPCR Master Mix (iQ SYBR Green Supermix; Bio-Rad) and each primer at 0.3 μM. Thermal amplification was carried out on a DNA Engine Opticon 2 real-time PCR detection system (Bio-Rad) according to the following conditions: 95°C for 10 minutes, followed by 45 cycles of 95°C for 15 seconds and 60°C for 60 seconds. Each sample was amplified in triplicate. Melt curve analysis for all the primer sets was performed to confirm the presence of a single product. Real-time PCR products were quantified and threshold cycle (Ct) numbers were automatically determined by iQ software (Bio-Rad). For data interpretation, we used the comparative ΔCt method as described by Livak and Schmittgen (31). The ΔCt values are the differences in the threshold cycles (Ct) for target and reference; therefore ΔCt = Ct (integrated retroviral DNA) – Ct (β-actin). No amplification was observed when genomic DNA from uninfected cell lines was used as template in real-time PCRs.

Semiquantitative Reverse Transcription–Polymerase Chain Reaction

Total RNA was isolated from cultured 0147T cells infected with retroviruses that expressed control shRNA, shRNAHN1, shRNAHN4, or shRNAHN5 by using an RNeasy kit and RNase-free DNase (both from Qiagen, GmbH, Hilden, Germany) according to manufacturer's instructions. Single-stranded complementary DNA (cDNA) was synthesized from 1 μg of total RNA by using an iScript cDNA synthesis kit (Bio-Rad). The cDNA samples were serially diluted (1:5 and 1:20) and subjected to PCR amplification with forward and reverse primers specific for HPV16 *E6* and *E7* cDNA sequences and for β-actin cDNA sequences and with *Taq*

Platinum polymerase (Invitrogen). Briefly, 1 μL of the diluted cDNA sample was added to a tube containing 1X reaction buffer (200 mM Tris–HCl [pH 8.4], 500 mM KCl, 1.5 mM $MgCl_2$), 100 μM of dATP, dTTP, dCTP and dGTP, 0.4 μM primer pair, and 1 U polymerase. PCR amplification of cDNA was performed under the following conditions: denaturation at 95°C for 5 minutes, followed by 27 cycles of 95°C for 30 seconds, 57°C for 30 seconds, and 72°C for 30 seconds. PCR primers used for the detection of E6, E7, and β-actin cDNAs were as follows: 16*E6* and *E7*F (5′-TCATGCATGGAGATACACCTACAT-3′), 16*E6* and *E7*R (5′-TGGTTTCTGAGAACAGATGG-3′), β-actinF (5′-CTCAC CATGGATGATGATAT-3′), and β-actinR (5′-TGGGTCAT CTTC-TCGCGGTT-3′). Amplified products were separated on a 1.5% agarose gel containing ethidium bromide and observed with a UV transilluminator (wavelength = 300 nm).

Quantitative Real-Time Reverse Transcription–Polymerase Chain Reaction

HPV16-positive oropharyngeal cancer cell lines (147T and 090) were infected with concentrated RV-shRNAHN4 retroviral stock as described above and then cultured for 48 hours. DNA-free total RNA was then extracted from the infected cells with the use of an RNeasy mini kit and RNase-free DNase (Qiagen) according to manufacturer's instructions. Total RNA (1 μg) was converted to cDNA by using the iScript cDNA synthesis kit (Bio-Rad) according to the manufacturer's instructions. Quantitative real-time reverse transcription–polymerase chain reaction (RT-PCR) was performed in separate 20-μL reaction volumes to evaluate expression of the *CDKN1A* (cyclin-dependent kinase inhibitor 1A, p21), *FAS* (tumor necrosis factor [TNF] receptor superfamily, member 6), *DEK* (DEK oncogene), *MYBL2* (v-myb myeloblastosis viral oncogene homolog-like 2, b-myb), HPV16 *E7*, and *GAPDH* (glyceraldehyde-3-phosphate dehydrogenase) genes. Quantitative PCRs were performed in triplicate with 40 ng of cDNA as template, the gene-specific forward and reverse primers (0.3 μM each; see Table 2 for sequences), hot-start iTaq DNA polymerase (Bio-Rad), and the iQ SYBR Green supermix (Bio-Rad) in a single-color icycler iQ Real-Time PCR detection system (Bio-Rad). The amplification program for all primer sets was 95°C for 3 minutes, followed by 40 cycles of 95°C for 10 seconds and 60°C for 90 seconds. Real-time PCR amplification data were analyzed and threshold cycle (Ct) numbers were automatically determined by iQ software (Bio-Rad). The relative expression of each mRNA was calculated by the comparative ΔCt method (31). Endogenous GAPDH mRNA levels were used for normalization of RNA expression.

Immunoblot Analysis

Protein extracts were prepared from uninfected and RV-shRNAHN4– or RV-control shRNA–infected 040T, 147T, and 090 cell lines as described previously (32,33). Total protein concentration was measured with a bicinchoninic acid assay kit (Bio-Rad) that used bovine serum albumin as a standard, according to the manufacturer's instructions. For electrophoresis, approximately 25 μg of protein per lane was resolved on 12% SDS–polyacrylamide gels and transferred to Immun-Blot PVDF membranes (Bio-Rad). Membranes were incubated with a mouse monoclonal antibody against human p53 protein (clone DO-7, 1:2000 dilution; DAKO, Carpinteria, CA); mouse monoclonal antibody against human pRb at 1:2000 dilution (clone 1F8; Lab Vision Corp, Freemont, CA); mouse monoclonal antibody against human p21 at 1:2000 dilution (sc-187; Santa Cruz Biotechnology, Santa Cruz, CA), and a mouse monoclonal antibody against human GAPDH at 1:2000 dilution (sc-59541; Santa Cruz Biotechnology). Bound antibody was detected by enhanced chemiluminescence (Amersham Biosciences).

Cell Viability Assays

Flow Cytometry. Uninfected and RV-shRNAHN4– or RV-control shRNA–infected 147T and 090 cells were cultured in 6-cm dishes (2×10^4 cells per dish). At 72 hours after infection, floating cells in the medium and adherent cells were collected and combined. The cells were stained with fluorescein isothiocyanate (FITC)–conjugated annexin V (annexin V–FITC) and propidium iodide (PI) with the use of an Annexin V–FITC Apoptosis detection kit (PharMingen, San Diego, CA), according to the manufacturer's instructions and analyzed by flow cytometry with the use of a FACS Calibur flow cytometer (Becton Dickinson, Franklin Lakes, NJ) at the Yale School of Medicine Core Research Facilities. The data were acquired using CellQuest V.3.3 software (BD Biosciences).

Water-Soluble Tetrazolium Salt Colorimetric Assay. We infected 090 cells with retroviruses expressing the shRNAHN4 or control shRNA as described above. Two days after infection, the cells were trypsinized, seeded in a 96-well plate (2×10^4 cells per well), and cultured for 3 days. Water-soluble tetrazolium salt reagent (Roche, Mannheim, Germany) was added to the growth medium (final dilution 1:10) for the 2 hours as described in the manufacturer's instruction manual, and viable cell mass was determined by the optical

Table 2. Sequences of primers for quantitative real-time reverse transcription–polymerase chain reaction*

Gene	Forward primer (5′ to 3′)	Reverse primer (5′ to 3′)
HPV16 *E7*	GCATGGAGATACACCTACATTG	TGGTTTCTGAGAACAGATGG
CDKN1A	ATTAGCAGCGGAACAAGGAGTCAGACATTT	GGCCAGTATGTTACAGGAGCTGGAAGGT
FAS	TGAAGGACATGGCTTAGAAGTG	GGTGCAAGGGTCACAGTGTT
DEK	AAACCTAGCCAGCTTCACGA	AGCCCCAACTCCAGAGAAAC
MYBL2	GCCACTTCCCTAACCGCAC	CCCTTGACAAGGTCTGGATTCA
GAPDH	CTGCACCACCAACTGCTTAG	GAAGATGGTGATGGGATTTC

* *CDKN1A* = cyclin-dependent kinase inhibitor 1A; *FAS* = tumor necrosis factor receptor superfamily member 6; *DEK* = DEK oncogene; *MYBL2* = v-myb myeloblastosis viral oncogene homolog-like 2; *GAPDH* = glyceraldehyde-3-phosphate dehydrogenase.

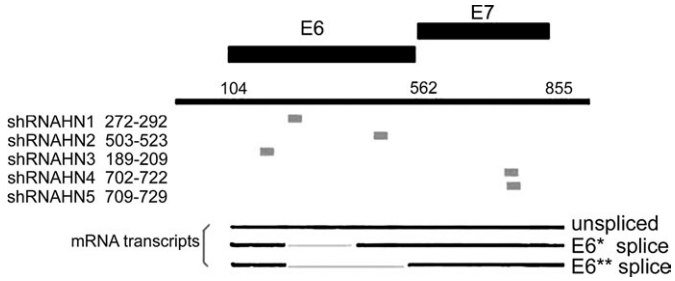

Figure 1. Short hairpin RNAs (shRNAs) designed to target regions throughout the full-length transcript encoding human papillomavirus type 16 (HPV16) *E6* and *E7*. The three alternate splicing patterns for HPV *E6* and *E7* mRNA are presented: unspliced = full-length mRNA; E6* splice = mRNA lacking nucleotides 226–410; and E6** splice = mRNA lacking nucleotide 226–526. The full-length transcript is designated by the **black line**. *E6* and *E7* coding regions are shown by **black rectangles**. Nucleotides 104 and 562 are the starting positions of the *E6* and *E7* coding regions, respectively, whereas nucleotide 855 is the end of E7 coding region. Target regions of shRNAs throughout the HPV16 *E6* and *E7* transcript are indicated by **gray rectangles**. Numbering is according to Seedorf et al. (29).

density measurement with the use of a FLUOstar OPTIMA microplate reader (BMG Labtech GmbH, Offenburg, Germany) at 420 nm and with 600 nm as a reference wavelength.

Senescence-Associated β-Galactosidase Assay. We cultured 040T and 090 cells infected with retroviruses expressing control shRNA or shRNAHN4 at 1.5×10^3 cells per cm^2 on 35-mm culture dishes for 15 days. Subsequently, cells were washed twice with phosphate-buffered saline (PBS) and fixed with 3% paraformaldehyde in PBS for 5 minutes at 4°C. The cells were washed three times with PBS, covered with a solution containing 5-bromo-4-chloro-3-indolyl-β-=-galactopyranoside at 1 mg/mL, 40 mM citric acid–sodium phosphate (pH 6.0), 5 mM potassium ferrocyanide, 5 mM potassium ferricyanide, 150 mM NaCl, and 2 mM $MgCl_2$ and incubated at 37°C overnight. The cells were rinsed twice with sterile water the following day and were examined by light microscopy for those that exhibited a medium- to dark-blue stain, indicative of senescence-associated β-galactosidase (SA-β-gal) activity (22).

Terminal Deoxynucleotidyltransferase–Mediated UTP End-Labeling Assay

We cultured 040T and 147T cells that had been infected with retroviruses expressing control shRNA or shRNAHN4 on culture slides (BD Biosciences) 2 days after retroviral infection. The following day, the cells were processed for the detection of DNA strand breaks with the use of an in situ cell death detection kit that included an Alexa Fluor 488 dye–labeled anti-BrdU antibody (MP23210; Molecular Probes, Invitrogen, Carlsbad, CA) according to the manufacturer's instructions for adherent cells. Briefly, the cells were washed with PBS and fixed with 1% (wt/vol) paraformaldehyde in PBS for 15 minutes at 4°C, washed with PBS, and stored in ice-cold 70% (vol/vol) ethanol for 1 hour. The cells were then incubated for 1 hour at 37°C in terminal deoxynucleotidyl transferase (TdT) solution, which contained reaction buffer, 5-bromo-2′-deoxyuridine-5′-triphosphate, and terminal deoxynucleotidyltransferase. The reactions were stopped by washing the slides with standard saline citrate buffer (0.03 M sodium citrate and 0.3 M sodium chloride). Slides were incubated with Alexa Fluor 488 dye–labeled anti-BrdU antibody for 30 minutes at room temperature. Nuclei were counterstained with 4,6-diamidino-2-phenylindole (DAPI). Fluorescent images of randomly chosen fields of cells were captured under fluorescence microscopy using a cooled CCD digital camera (Photometrics series CC200, Tuscon, AZ) in both the DAPI fluorescence channel and the Alexa Fluor 488 dye fluorescence channel.

Results

Effect of shRNA-Mediated Suppression of HPV *E7* and *E6* Gene Expression in HPV16-Positive Oropharyngeal Cancer Cells

To disrupt HPV *E6* and *E7* gene expression, we designed five shRNA oligonucleotides that targeted various locations within the HPV16 *E6* and *E7* transcript (Figure 1). We used a retrovirus-mediated gene-specific shRNA knockdown system to clone these oligonucleotides into an shRNA expression vector, and high-titer retroviruses expressing the shRNA knockdown constructs were generated in 293T cells. These retroviruses were used to infect HPV16-positive (147T and 090) and HPV-negative (040T) oropharyngeal cancer cell lines. Two days after infection, we used quantitative RT-PCR analysis to analyze the expression of HPV16 *E6* and *E7* mRNA. In 147T (Figure 2, A) and 090 (data not shown) cells, expression of the five HPV16 *E6* and *E7*–targeting shRNAs reduced the *E6* and *E7* mRNA levels (normalized to that of GAPDH mRNA) by 56% to more than 85% compared with *E6* and *E7* mRNA levels of control cells that expressed a scrambled-sequence shRNA. The scrambled shRNA had no effect on *E6* and *E7* mRNA levels in either of the HPV16-positive cell lines compared with uninfected cells (data not shown). Infection with retroviruses expressing two shRNAs (shRNAHN4 and shRNAHN5) showed the highest silencing efficiency, causing an approximately 10-fold knockdown of HPV16 *E6* and *E7* mRNA levels compared with uninfected cells (mean fold change of *E6* and *E7* mRNA in RV-shRNAHN4–infected 147T cell line vs uninfected 147T cell line = 0.110, 95% confidence interval [CI] = 0.106 to 0.114, $P < .001$; mean fold change of *E6* and *E7* mRNA in RV-shRNAHN5–infected 147T cell line vs uninfected 147T cell line = 0.08, 95% CI = 0.077 to 0.084, $P < .001$), whereas infection with retroviruses expressing the other three shRNA oligonucleotides caused an approximately fivefold knockdown (Figure 2, A). The real-time PCR data on silencing efficiency were also confirmed by semiquantitative PCR (Figure 2, B). We used the retrovirus that resulted in the greatest reduction in *E6* and *E7* mRNA levels in infected cells—RV-shRNAHN4—for subsequent experiments. To confirm that retroviral infection efficiency was almost the same for the HPV-positive and HPV-negative cell lines included in our quantitative RT-PCR analysis, we performed real-time PCR to amplify the integrated viral DNA and the β-actin gene (internal reference) from genomic DNA isolated from RV-shRNAHN4–infected 040T, 147T, 090, and SiHa cells 48 hours after infection. Uninfected cells (040T, 147T, 090, and SiHa) were included in this analysis as negative controls. All samples subjected to real-time PCR analysis contained the same amount of input genomic DNA (100 ng). Real-time PCR data analysis showed that the retroviral DNA amplicon was efficiently amplified in samples from retrovirus-infected cell lines, whereas retroviral DNA

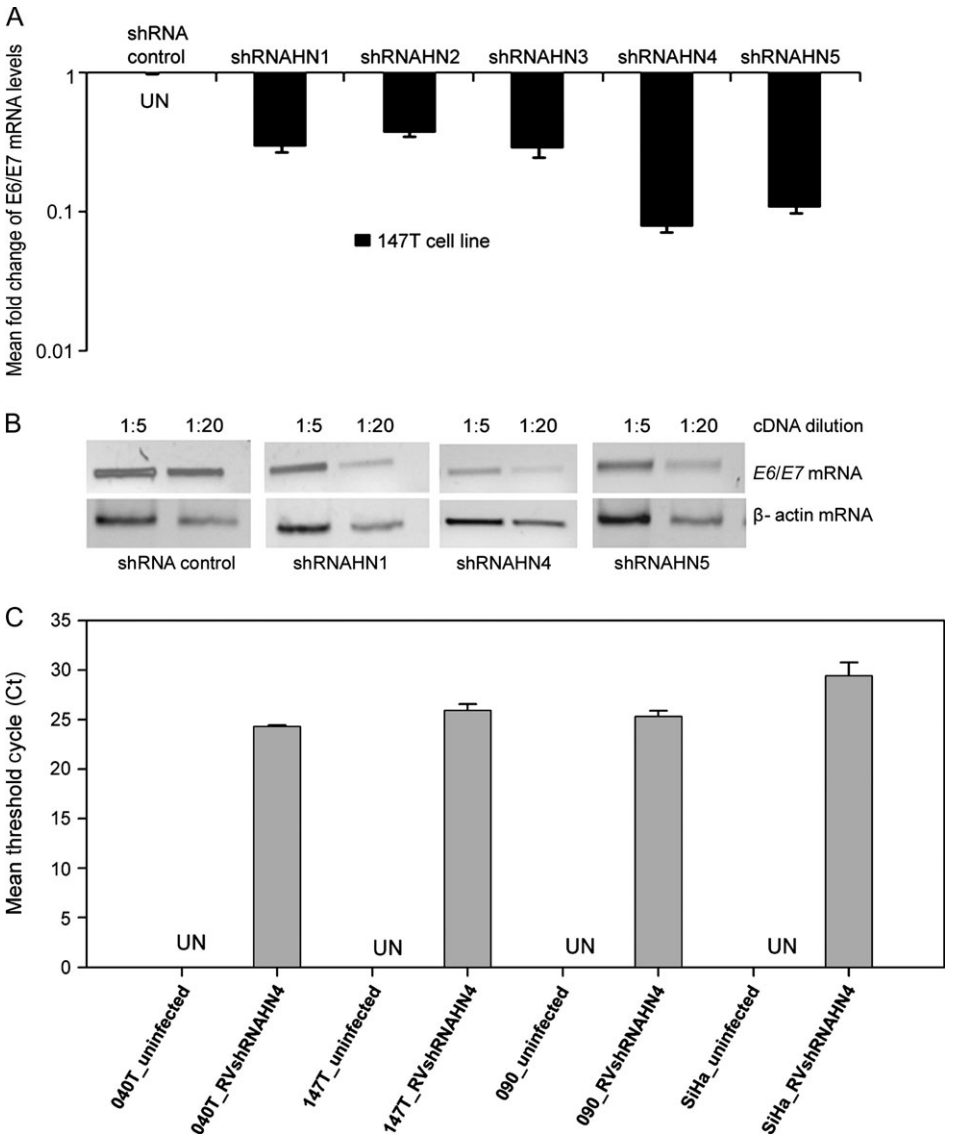

Figure 2. Effect of short hairpin RNA (shRNA) expression on human papillomavirus type 16 (HPV16) *E6* and *E7* mRNA expression in 147T cells. **A**) Silencing efficiency of shRNA oligonucleotides by quantitative real-time reverse transcription–polymerase chain reaction (RT-PCR). The 147T cells were infected with retroviruses expressing shRNAs targeting the *E6* and *E7* mRNA (shRNAHN1–5) or control retroviruses expressing scrambled-sequence shRNAs. Twenty-four hours after infection, total RNA was extracted from infected cells and reverse transcribed to generate complementary DNA (cDNA), which was diluted and subjected to real-time PCR amplification of the viral *E6* and *E7* transcript. Mean fold change of *E6* and *E7* mRNA levels compared with *E6* and *E7* mRNA levels of uninfected 147T cells (set as 1 on the vertical axis) were calculated for each sample and plotted. Quantitative PCRs were performed in triplicate. **Error bars** = 95% confidence intervals; UN = undetectable. **B**) Silencing efficiency of shRNA oligonucleotides by semiquantitative RT-PCR. 147T cells were infected by retroviruses expressing the indicated shRNAs. Two days after infection, cytoplasmatic RNA was extracted from the infected cells and reverse transcribed to generate cDNA, which was diluted 1:5 and 1:20 and subjected to PCR amplification of HPV16 *E6* and *E7* and β-actin mRNAs. PCR products were separated by electrophoresis on a 1.5% agarose gel containing ethidium bromide and visualized by UV irradiation. **C**) Relative integration efficiency of retrovirus DNA in oropharyngeal cell lines. 040T, 147T, and 090 cells were infected with retroviruses expressing the shRNAHN4 (RV-shRNA4). Twenty-four hours after infection, genomic DNA (100 ng) from infected and uninfected cells was used as template for real-time PCR for the quantification of integrated virus DNA. Mean threshold cycle (Ct) values are shown. The threshold cycle corresponds to the cycle number at which the fluorescence generated crosses the threshold. Quantitative PCRs were performed in triplicate. **Error bars** = 95% confidence intervals; UN = undetectable.

amplification was not detected in samples from uninfected cell lines. As shown in Figure 2, C, mean threshold cycle (Ct) values for integrated retroviral DNA were comparable between HPV-positive (147T, 090, and SiHa) and HPV-negative (040T) cell lines. Because the mean Ct values for β-actin (the internal reference) amplification were almost identical for all the samples analyzed, this assay confirmed that transfection and integration efficiency of viral DNA was comparable across the infected cell lines.

Biochemical Analysis of Retrovirus-Infected Oropharyngeal Squamous Cell Cancer Cell Lines

We next examined the biochemical responses of the oropharyngeal squamous cell cancer cells to shRNA-mediated repression of HPV16 *E6* and *E7* expression. We specifically examined the effects of *E6* and *E7* gene silencing on the mRNA and protein expression levels of components of the p53 and Rb tumor suppressor pathways. Immunoblot analysis of protein extracts prepared 48 and 72 hours after retrovirus infection with an antibody specific for p53 revealed a marked increase in the level of p53 protein in shRNAHN4-infected (HPV-positive) 147T and 090 cells compared with the levels of p53 protein in uninfected or RV-shRNA control–infected 147T and 090 cell lines, presumably as the result of shRNA-mediated repression of HPV16 *E6* gene expression and the loss of E6-induced destabilization of p53 (Figure 3, A and B). By contrast, RV-shRNAHN4 infection of HPV-negative 040T cells did not increase the level of p53 compared with uninfected cells (Figure 3, A and B). To investigate the possible activation of p53 pathway by shRNA-mediated repression of HPV16 *E6* and *E7* expression, we used quantitative RT-PCR to examine the expression of two p53-activated genes—*p21* and *FAS*—48 hours after RV-shRNAHN4 infection of 147T and 090 cells. This analysis revealed rapid increases in the levels of p21

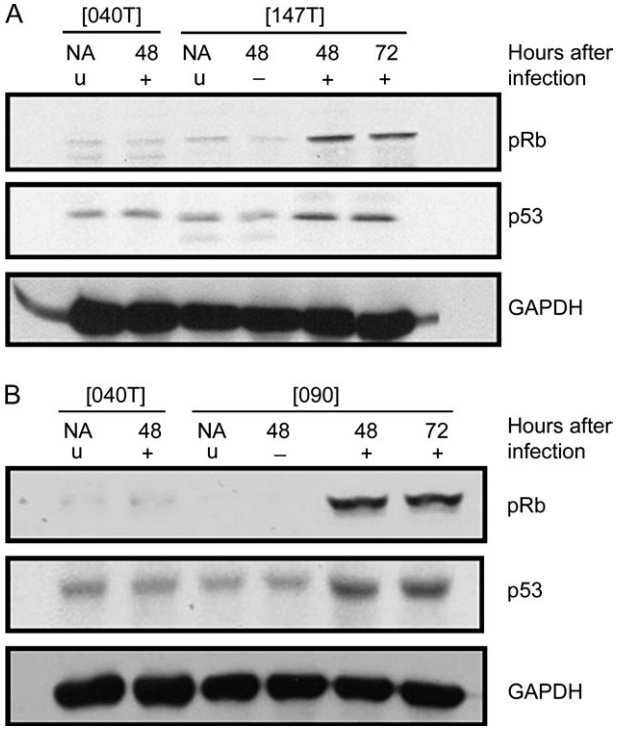

Figure 3. Effect of short hairpin RNA (shRNA)–mediated repression of human papillomavirus type 16 *E6* and *E7* on p53 and retinoblastoma (pRb) expression. **A**) Immunoblot analysis of p53 and pRb protein levels in 147T cells. **B**) Immunoblot analysis of p53 and pRb protein levels in 090 cells. Protein extracts were made from uninfected (u) 147T, 040T, and 090 cells and from cells that were infected for 48 hours (147T, 040T, and 090 cells) or 72 hours (147T and 090 cells) with retrovirus expressing shRNAHN4 (+) or the scrambled-sequence control shRNA (−). Extracted protein samples (25 μg per lane) were subjected to electrophoresis and immunoblotting with antibodies specific for $p105^{Rb}$, p53, and glyceraldehyde-3-phosphate dehydrogenase (GAPDH) as control for equal loading. NA = not applicable.

and FAS mRNAs. More specifically, p21 mRNA levels increased fourfold in infected 147T cells and threefold in infected 090 cells and *FAS* mRNA levels increased threefold in infected 147T and 090 cells, all compared with RV-shRNA control–infected cells (mean fold change of p21 mRNA in RV-shRNAHN4–infected 147T cell line vs RV-shRNA control 147T cell line = 4.08, 95% CI = 3.97 to 4.19, $P < .001$; mean fold change of p21 mRNA in RV-shRNAHN4–infected 090 cell line vs RV-shRNA control–infected 090 cell line = 3.25, 95% CI = 3.2 to 3.3, $P < .001$; mean fold change of *FAS* mRNA in RV-shRNAHN4–infected 147T cell line vs RV-shRNA control 147T cell line = 2.96, 95% CI = 2.91 to 3.01, $P < .001$; mean fold change of *FAS* mRNA in RV-shRNAHN4–infected 090 cell line vs RV-shRNA control–infected 090 cell line = 2.91, 95% CI = 2.83 to 2.99, $P < .001$) (Figure 4, A). Increased expression of the p21 protein in these cells after infection was also confirmed by immunoblot analysis (Figure 4, B). We did not observe any change in expression of *p21* or *FAS* in RV-control shRNA–infected or uninfected 147T and 090 cells (data not shown).

Infection of 147T and 090 cell lines with retrovirus expressing shRNAHN4 caused a marked increase in the level of pRb, presumably because of repression of endogenous HPV16 E7 expression in these cells and the loss of E7-mediated destabilization of pRb (Figure 3, A and B). pRb regulates the activity of E2F transcription factors, and complexes consisting of E2F and hypophosphorylated pRb repress the transcription of genes such as cyclin A that are required for cell cycle progression. The E7 protein expressed by high-risk HPVs binds to Rb family members and disrupts Rb–E2F complexes, resulting in increased expression of E2F-responsive genes, many of which are required for cell cycle progression (18–20). To investigate the possible activation of the pRb suppressor pathway in response to E7 suppression, we used quantitative RT-PCR to analyze the expression of two well-described E2F-target genes—*DEK* and *B-MYB* (18)—in control RV-shRNA– and RV-shRNAHN4–infected 147T and 090 and 040 cell lines. This analysis revealed that DEK and B-MYB mRNA levels were substantially reduced in RV-shRNAHN4–infected 147T and 090 cells compared with control shRNA–infected 147T and 090 cells or cells devoid of HPV DNA (040T) (mean fold change of DEK mRNA in RV-shRNAHN4–infected 147T cell line vs RV-shRNA control 147T cell line = 0.43, 95% CI = 0.407 to 0.452, $P < .001$; mean fold change of DEK mRNA in RV-shRNAHN4–infected 090 cell line vs RV-shRNA control–infected 090 cell line = 0.32, 95% CI = 0.302 to 0.337, $P < .001$; mean fold change of B-MYB mRNA in RV-shRNAHN4–infected 147T cell line vs RV-shRNA control 147T cell line = 0.11, 95% CI = 0.10 to 0.12, $P < .001$; mean fold change of B-MYB mRNA in RV-shRNAHN4–infected 090 cell line vs RV-shRNA control–infected 090 cell line = 0.46, 95% CI = 0.425 to 0.495, $P < .001$) (Figure 4, A). The decreased expression of DEK and B-MYB mRNA was likely due to the restoration of pRb expression, which would have formed complexes with E2F transcription factors that subsequently repressed the transcription of these genes. When 147T and 090 cells were infected with the control retrovirus expressing a scrambled-sequence shRNA, the expression of both DEK and B-MYB mRNA was similar to their expression in uninfected cells (data not shown). Similarly, infection of the HPV-negative 040T cell line with RV-shRNAHN4 caused no change in $p105^{Rb}$ levels compared with uninfected cells (Figure 3). Taken together, these results indicate that repression of the HPV16 *E6* and *E7* oncogenes in HPV16-positive oropharyngeal cancer cells leads to activation of the p53 and pRb tumor suppressor pathways.

Phenotypic Effects of HPV16 *E6* and *E7*–Targeting shRNAs in 147T and 090 Cells

We observed substantial morphological changes in HPV-positive 147T cells infected with RV-shRNAHN4 by 2 days after infection compared with 147T cells infected with the control RV-shRNA or RV-shRNAHN4–infected HPV-negative 040T cells. The RV-shRNAHN4–infected 147T cells shriveled, detached from the plate, and died (data not shown). Similar morphological changes, as well as cell death, were also observed in RV-shRNAHN4–infected 090 cells, but to a lesser extent (data not shown).

Data from previous studies showed that repression of HPV16 *E6* and *E7* oncogenes in cervical cancer cells results in apoptosis (33), senescence (22), or both (34). We examined whether the loss of cell viability that we observed in RV-shRNAHN4–infected 147T cells was via apoptosis by using flow cytometry to assess

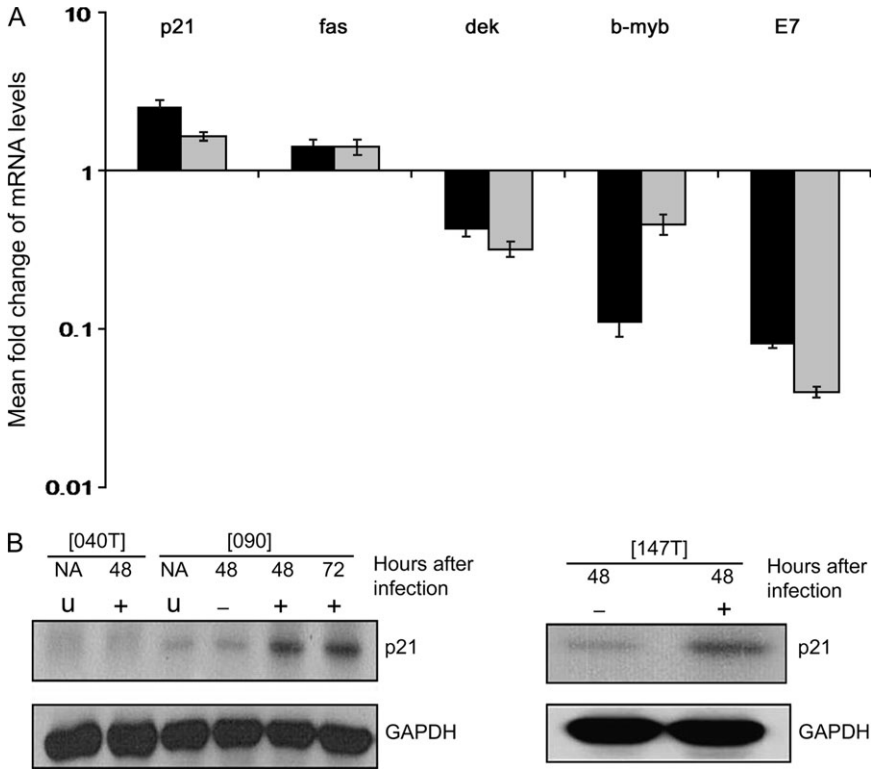

Figure 4. Expression of selected p53- and E2F-activated genes in RV-shRNAHN4–infected 147T and 090 cells. **A**) Quantitative real-time reverse transcription–polymerase chain reaction (qRT-PCR) analysis. RNA was harvested 72 hours after RV-shRNAHN4 infection of 147T (**black bars**) and 090 (**gray bars**) cells and subjected to gene expression analysis by qRT-PCR. Fold change in gene expression (normalized to glyceraldehyde-3-phosphate dehydrogenase gene [GAPDH] expression) was compared with cells infected with retrovirus expressing the scrambled-sequence control short hairpin RNA (shRNA). Levels of mRNA in control infected (RV-shRNA control) cells are set at 1 on the vertical axis. Values greater than 1 represent a fold increase in mRNA expression levels, whereas values less than 1 represent a fold decrease in mRNA expression levels. Quantitative PCRs were performed in triplicate. **Error bars** = 95% confidence intervals. For all genes analyzed, the mean fold change in mRNA level between the RV-shRNAH4–infected cells (147T or 090) and the corresponding RV-control shRNA–infected cells was statistically significant ($P < .001$, two-sided t test). **B**) Immunoblot analysis of p21 expression. Protein extracts made from uninfected (u) 040T and 090 cells and from 040T, 090, and 147T cells infected for 48 or 72 hours with retrovirus expressing shRNAHN4 (+) or retrovirus expressing control shRNA (−) were subjected to electrophoresis (25 μg per lane) and immunoblotting with an antibody specific for p21. Glyceraldehyde-3-phosphate dehydrogenase (GAPDH) expression was used as a control for equal protein loading. NA = not applicable.

annexin V binding and PI permeability of nonpermeabilized 147T and 090 cells 2 days after infection with retrovirus expressing the control shRNA or shRNAHN4 (Figure 5). Infection with RV-shRNAHN4 increased the percentage of annexin V–positive cells (upper and lower right quadrants combined) from 13.4% in uninfected 147T cells to 84.3% in RV-shRNAHN4–infected 147T cells (Figure 5, A) and from 3.3% in uninfected 090 cells to 71.2% in RV-shRNAHN4–infected 090 cells (Figure 5, C). Most of the annexin V–positive cells were also positive for propidium iodine in both cell lines, indicating that apoptosis is initiated rapidly after *E6* and *E7* silencing in RV-shRNA4–infected HPV16-positive cell lines and by 3 days after infection, cells are in a late phase of apoptosis. The cell viability assay showed a pronounced reduction in viability (>50%) of RV-shRNAHN4–infected HPV-positive 090 cells, 96 hours after retrovirus infection compared with control RV-shRNA–infected 090 cells. By contrast, the viability of the RV-shRNAHN4–infected HPV-negative cell line (040T) was almost identical to that of control RV-shRNA–infected 040 cells (Figure 5, D).

We also used terminal deoxynucleotidyltransferase–mediated UTP end-labeling (TUNEL) staining to examine the retrovirus-infected cells for DNA fragmentation, another marker of apoptosis. At 72 hours after infection, RV-shRNAHN4–infected 147T cells exhibited a massive induction of apoptosis, as indicated by the substantial number of TUNEL-positive cells compared with control RV-shRNA–infected cells (Figure 6). To confirm the specificity of cell killing induced by RV-shRNAHN4, we infected two HPV-positive cervical carcinoma cell lines—HeLa (HPV18 positive) and SiHa (HPV16 positive)—with the control shRNA– and shRNAHN4-expressing retroviruses and subjected them to TUNEL staining 72 hours after infection. Unlike SiHa cells, HeLa cells were not killed by shRNAHN4 infection even at high doses (data not shown), suggesting that the apoptotic response seen in HPV16-positive cell lines following infection with retrovirus targeting HPV16 *E6* and *E7* was specific and due to HPV16 *E6* and *E7* gene silencing. These results clearly demonstrate that RV-shRNAHN4 infection induced an apoptotic response that was specific for the HPV16-positive cancer cells.

Finally, we examined whether RV-shRNAHN4 infection induced senescence in 147T and 090 cells by assaying the cells 15 days after infection for the expression of SA-β-gal, a well-described marker for cellular senescence that results from induction of lysosomal acid β-galactosidase activity (35,36). We did not observe SA-β-gal–positive cells in these cultures. This result suggests that repression of endogenous *E6* and *E7* proteins in 147T and 090 cells causes the cells to undergo apoptosis rather than senescence.

Discussion

In this study, we showed that shRNA-mediated repression of HPV16 *E6* and *E7* oncogene expression resulted in activation of the p53 and pRb tumor suppressor pathways and induction of apoptosis in HPV16-positive oropharyngeal cancer cell lines. These results suggest that continuous expression of HPV *E6* and *E7* in HPV16-positive human oropharyngeal cancer cells is required to maintain the malignant phenotype and actively prevent the execution of apoptosis.

Establishing a link between head and neck cancer and HPV infection has been difficult. According to a meeting report on modern criteria to establish cancer etiology (13), establishing a causal relationship requires information from epidemiology and molecular pathology together with experimental evidence. Epidemiological

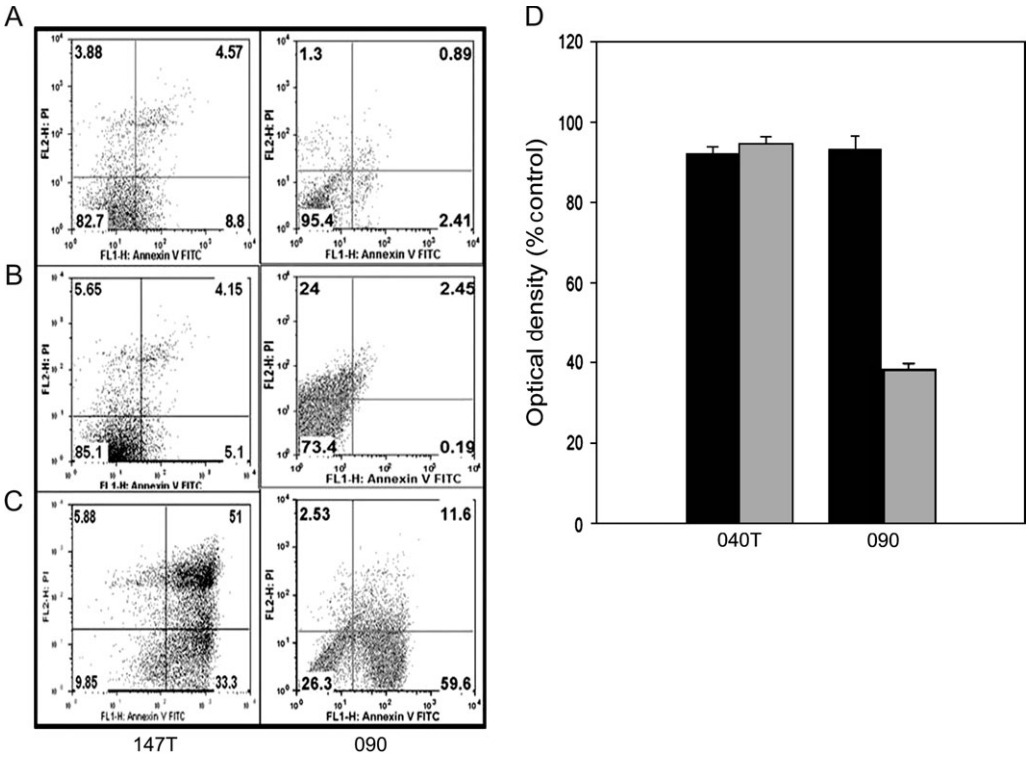

Figure 5. Effect of human papillomavirus type 16 *E6* and *E7* repression on apoptosis. **A**) Unfixed uninfected 147T and 090 cells. **B**) 147T and 090 cells infected with retroviruses expressing control short hairpin RNA (shRNA). **C**) 147T and 090 cells infected with retroviruses expressing shRNAHN4. Cells were assayed by flow cytometry for annexin V binding and propidium iodine staining 72 hours after infection. The logarithm of annexin V–fluorescein isothiocyanate fluorescence and the logarithm of propidium iodide (PI) fluorescence were plotted on the *x* and *y* axes of the cytogram. The lower right quadrant shows the percentage of viable cells in the early stages of apoptosis (ie, annexin V–positive, PI-negative cells), the upper right quadrant shows the percentage of cells in a later stage of apoptosis or necrosis (annexin V–positive, PI-positive cells), the lower left shows the percentage of cells in the proliferating-senescence state and the upper left quadrant shows the percentage of dead cells. **D**) Effect of *E6* and *E7* repression on 040T and 090 cell viability. 040T and 090 cells were infected with retroviruses expressing shRNAHN4 (**shaded bars**) or control shRNA (**black bars**). Two days after infection, the cells were trypsinized and seeded in a 96-well plate (2×10^4 cells per well). Cell viability was measured with the use of the water-soluble tetrazolium salt colorimetric assay 96 hours after retrovirus infection. Viability was determined by measuring the optical density at 420 nm (with 600 nm as a reference wavelength) and is expressed as the mean percentage of the viability of uninfected cells for each cell line (set at 100%). Mean values for three independent experiments are plotted. **Error bars** = 95% confidence intervals.

studies have shown an association between high-risk HPVs and oropharyngeal cancers in individuals who engage in sexual activities associated with viral transmission (3). Molecular pathology studies have detected high-risk HPVs in oropharyngeal cancers (2,4). This study provides one of the missing pieces of experimental evidence in that it demonstrates that continuous expression of the *E6* and *E7* oncogenes is required for the maintenance of the proliferative state of HPV16-positive oropharyngeal cancer cells. HPV16-positive oropharyngeal cancer cells are similar to HPV16-positive cervical cancer cells in that they contain the genes encoding wild-type p53 and pRb but fail to express these proteins because of the continuous expression of the *E6* and *E7* gene, respectively. Ferris et al. (27) also showed restoration of p53 protein expression after repression of E6 in the 090 cell line.

Despite the large body of epidemiological and molecular pathology data showing an association between HPV16 and a subset of oropharyngeal cancers, the role of HPV in oropharyngeal cancer progression is not as well defined as it is in cervical cancer. Molecular pathology studies have shown that HPV DNA is present in oropharyngeal cancers (2,4). However, detection of HPV DNA in oropharyngeal cancer tissue per se does not prove a causal association. Moreover, only a small fraction of HPV-infected individuals develop cancer. Most studies in oropharyngeal cancer suggest that tumors that are positive for transcriptionally active HPV share similar molecular features to cervical cancer, namely a wild-type p53 gene, low levels of pRb, and high levels of p16 (37,38). However, HPV DNA–positive oropharyngeal tumors bearing p53 gene mutations have also been described (39). The presence of p53 mutations in a subset of HPV DNA–positive head and neck squamous cell carcinomas challenged an etiological role of the virus in oropharyngeal squamous cell cancer. The existence of a subgroup of oropharyngeal cancers that is HPV positive and p53 mutant has been attributed to the fact that the HPV DNA, although present, is not transcribed in this subset of tumors (34). Therefore, E6 mRNA is not present in this subset of tumors and p53 is inactivated via mutations rather than as the result of E6-mediated degradation. A hit-and-run mechanism has also been proposed to explain the existence of HPV-positive oropharyngeal squamous cell carcinomas bearing p53 mutations, in which the virus plays a role only in the initial steps of carcinogenesis in this subset of tumors (40).

In this study, we used carcinoma cell lines that contain transcriptionally active HPV16. Our findings support the notion that oropharyngeal cancers that contain transcriptionally active HPV16 follow the same carcinogenic pathway as has been described in cervical carcinogenesis: inactivation of p53 and pRb tumors suppressor pathways occurs via degradation in response to expression of the *E6* and *E7* genes, respectively, and repression of these viral oncogenes restores these tumor suppressor pathways and leads to apoptosis.

In our experimental system, repression of *E6* and *E7* oncogenes led to apoptosis. By contrast, introduction of the BPV E2 gene into cervical carcinoma cell lines (HeLa) represses viral oncogene expression, resulting in either senescence (14) or apoptosis (23). In addition, in HeLa cells, E2-mediated repression of *E6* alone

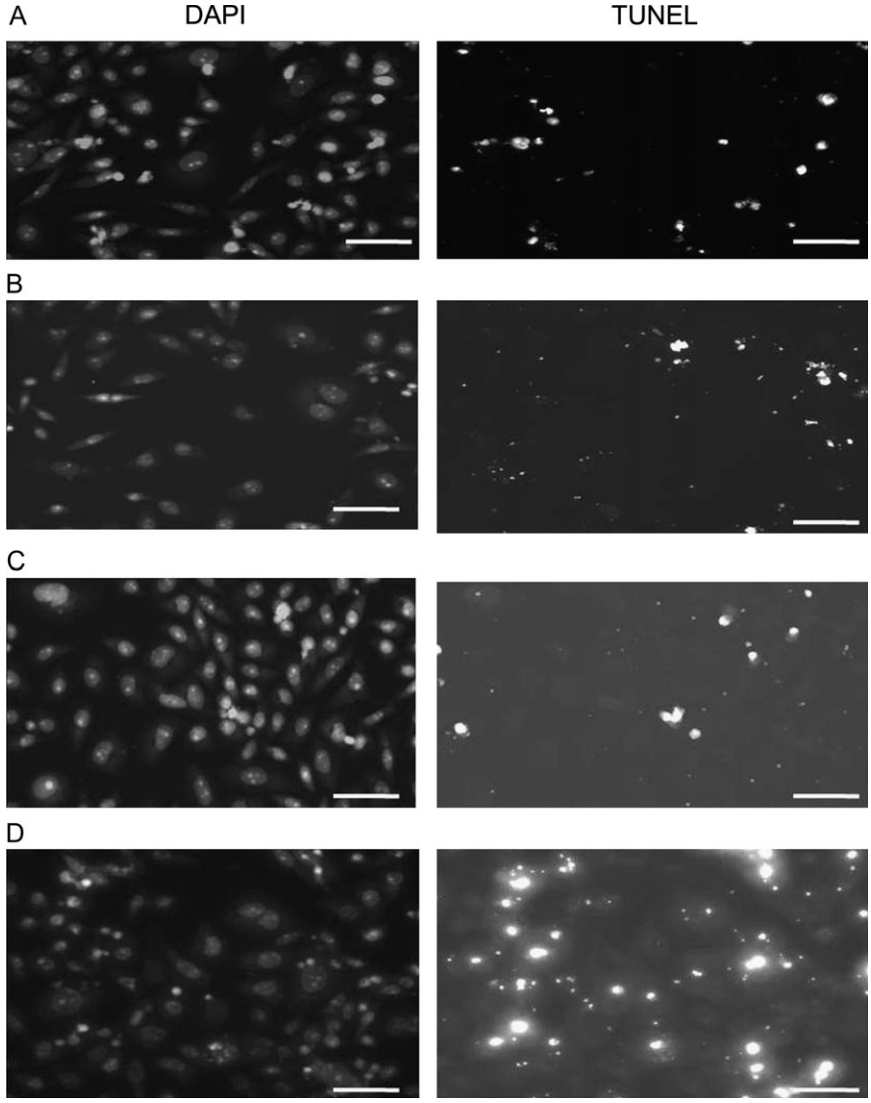

Figure 6. Terminal deoxynucleotidyltransferase–mediated UTP end-labeling (TUNEL) assay for the assessment of apoptosis in RV-shRNAHN4–infected 147T cells. **A**) 040T cells infected with retrovirus expressing shRNAHN4. **B**) Uninfected 147T cells. **C**) 147T cells infected with retroviruses expressing control short hairpin RNA. **D**) 147T cells infected with retrovirus expressing shRNAHN4. Uninfected and retrovirus-infected cells were fixed on culture slides (retrovirus-infected cells were fixed 72 hours after infection). The total DNA was stained with 4.6-diamidino-2-phenylindole (DAPI) and cells undergoing apoptosis were visualized under a fluorescence microscope after staining with digoxigenin dUTP antibody at ×40 magnification. **Scale bar** = 10 μm.

leads to apoptosis (34), whereas repression of E7 alone leads to senescence (41). Gu et al. (42) showed that low-multiplicity infection of HeLa cells with RV-shRNA targeting *E6* and *E7* induced senescence, whereas a high-multiplicity infection resulted in apoptotic cell death, indicating that the level of *E6* and *E7* mRNA expression is associated with the host cellular response. However, the specific factors that determine the cellular response to *E6* and *E7* repression remain unclear. The pattern of gene expression in response to the repression of *E6* and *E7* genes as well as the restoration of p53 and pRb expression that we observed in HPV16-positive oropharyngeal cancer cell lines was consistent with the observed apoptotic cellular response because several of the genes whose expression was altered are mediators of apoptosis. Of particular interest among these apoptotic mediators are genes that are direct transcriptional targets of p53 or pRb. The restoration of p53 expression stimulated a relatively rapid induction of p21, a well-known direct target of p53 (43,44). It is also interesting that Fas expression was increased after silencing of *E6* and *E7*. Fas is a cell surface protein member of the TNF receptor superfamily and is implicated in p53-dependent apoptosis (45,46). Specifically, Fas expression is stimulated by p53 via a p53-responsive element within the Fas promoter and first intron region (45,46). In addition to stimulation of Fas transcription, overexpressed p53 has been also shown to enhance levels of Fas at the cell surface by promoting translocation of the Fas receptor from the Golgi (47). Restoration of p53 expression has been found to sensitize HPV16-immortalized human keratinocytes derived from adult skin and foreskins to Fas-mediated apoptosis (48). In this study, restoration of p53 levels 48 hours after *E6* and *E7* silencing was associated with an increase in *FAS* gene expression. Hence, Fas-triggered apoptosis may explain why we detected apoptotic cell death in a substantial fraction of the cell population in the HPV16-positive oropharyngeal cancer lines 48 hours after *E6* and *E7* silencing.

The high-risk HPV E7 protein binds to Rb family members and disrupts Rb–E2F complexes, resulting in increased expression of E2F-responsive genes, many of which are required for cell cycle progression (18–20). Therefore, we next sought to examine whether restoration of pRb protein expression following E7 silencing repressed mRNA levels of known E2F-target genes. To accomplish our goal, we analyzed the expression of transcriptional regulators DEK and B-MYB (49,50) at 0 and 48 hours after

shRNA-mediated silencing of the E7 gene. Our results showed a decreased expression of these genes, presumably because of the assembly of active Rb–E2F complexes after E7 silencing. Previous studies have shown that repression of either B-MYB or DEK can inhibit cell growth and survival (51,52). Wise-Drapper et al. (52) showed that DEK expression protects HPV-positive cancer cells and primary human cells from apoptotic cell death. They also found that DEK depletion was associated with increased p53 stability and transcriptional activity and the consequent increased expression of p53-targeted genes, such as p21 and Bax. B-MYB has also been shown to enhance cell survival by activating antiapoptotic genes such as *CLU* and *BCL2* (53,54). The simultaneous delivery of multiple apoptosis-inducing signals may account for the profound cell death caused by *E6* and *E7* repression.

According to the "Modern Criteria to Establish Human Cancer Etiology" (13), supportive experimental animal evidence (ie, regression of HPV16-positive tumors in animals following *E6* and *E7* repression) is also needed to ultimately prove causal association. Thus, a limitation of this study is that we performed only in vitro experiments showing that continuous expression of *E6* and *E7* HPV16 oncogenes is required for inactivation of p53 and Rb tumor suppressor pathways and the maintenance of the proliferative state of HPV16-positive oropharyngeal cancer cells.

In summary, this study provides experimental evidence that HPV16 is required for malignant transformation and survival of HPV16-positive oropharyngeal cancer cell lines. These results, along with epidemiological and molecular pathology studies, contribute to the establishment of a causal association between HPV and oropharyngeal cancer. Validation of a causal relationship, if followed by the rapid deployment of preventive and therapeutic strategies, such as anti-HPV vaccines, could have a major impact on public health.

References

1. Walboomers JM, Jacobs MV, Manos MM, et al. Human papillomavirus is a necessary cause of invasive cervical cancer worldwide. *J Pathol.* 1999;189(1):9–12.
2. Gillison ML, Koch WM, Capone RB, et al. Evidence for a causal association between human papillomavirus and a subset of head and neck cancers. *J Natl Cancer Inst.* 2000;92:709–720.
3. D'Souza G, Kreimer AR, Viscidi R, et al. Case-control study of human papillomavirus and oropharyngeal cancer. *N Engl J Med.* 2007;356: 1944–1956.
4. Andl T, Kahn T, Pfuhl A, et al. Etiological involvement of oncogenic human papillomavirus in tonsillar squamous cell carcinomas lacking retinoblastoma cell cycle control. *Cancer Res.* 1998;58:5–13.
5. Steinberg BM, DiLorenzo TP. A possible role for human papillomaviruses in head and neck cancer. *Cancer Metastasis Rev.* 1996;15:91–112.
6. Fakhry C, Gillison ML. Clinical implications of human papillomavirus in head and neck cancers. *J Clin Oncol.* 2006;24:2606–2611.
7. Frisch M, Hjalgrim H, Jaeger AB, Biggar RJ. Changing patterns of tonsillar squamous cell carcinoma in the United States. *Cancer Causes Control.* 2000;11:489–495.
8. Shiboski CH, Schmidt BL, Jordan RC. Tongue and tonsil carcinoma: increasing trends in the U.S. population ages 20–44 years. *Cancer.* 2005; 103:1843–1849.
9. Smith EM, Ritchie JM, Summersgill KF, et al. Age, sexual behavior and human papillomavirus infection in oral cavity and oropharyngeal cancers. *Int J Cancer.* 2004;108:766–772.
10. de Villiers EM, Weidauer H, Otto H, zur Hausen H. Papillomavirus DNA in human tongue carcinomas. *Int J Cancer.* 1985;36:575–578.
11. Schwartz SM, Daling JR, Doody DR, et al. Oral cancer risk in relation to sexual history and evidence of human papillomavirus infection. *J Natl Cancer Inst.* 1998;90:1626–1636.
12. Fakhry C, D'Souza G, Sugar E, et al. Relationship between prevalent oral and cervical human papillomavirus infections in human immunodeficiency virus-positive and -negative women. *J Clin Microbiol.* 2006;44: 4479–4485.
13. Carbone M, Klein G, Gruber J, Wong M. Modern criteria to establish human cancer etiology. *Cancer Res.* 2004;64:5518–5524.
14. Goodwin EC, DiMaio D. Repression of human papillomavirus oncogenes in HeLa cervical carcinoma cells causes the orderly reactivation of dormant tumor suppressor pathways. *Proc Natl Acad Sci USA.* 2000; 97:12513–12518.
15. Psyrri A, DeFilippis RA, Edwards AP, Yates KE, Manuelidis L, DiMaio D. Role of the retinoblastoma pathway in senescence triggered by repression of the human papillomavirus E7 protein in cervical carcinoma cells. *Cancer Res.* 2004;64:3079–3086.
16. Alani RM, Munger K. Human papillomaviruses and associated malignancies. *J Clin Oncol.* 1998;16:330–337.
17. Werness BA, Levine AJ, Howley PM. Association of human papillomavirus types 16 and 18 E6 proteins with p53. *Science.* 1990;248:76–79.
18. Munger K, Basile JR, Duensing S, et al. Biological activities and molecular targets of the human papillomavirus E7 oncoprotein. *Oncogene.* 2001; 20:7888–7898.
19. Serrano M, Hannon GJ, Beach D. A new regulatory motif in cell-cycle control causing specific inhibition of cyclin D/CDK4. *Nature.* 1993;366:704–707.
20. Dyson N. The regulation of E2F by pRB-family proteins. *Genes Dev.* 1998;12:2245–2262.
21. von Knebel Doeberitz M, Oltersdorf T, Schwarz E, Gissmann L. Correlation of modified human papilloma virus early gene expression with altered growth properties in C4-1 cervical carcinoma cells. *Cancer Res.* 1988;48:3780–3786.
22. Hall AH, Alexander KA. RNA interference of human papillomavirus type 18 *E6* and *E7* induces senescence in HeLa cells. *J Virol.* 2003;77: 6066–6069.
23. Desaintes C, Demeret C, Goyat S, Yaniv M, Thierry F. Expression of the papillomavirus E2 protein in HeLa cells leads to apoptosis. *Embo J.* 1997;16:504–514.
24. Dowhanick JJ, McBride AA, Howley PM. Suppression of cellular proliferation by the papillomavirus E2 protein. *J Virol.* 1995;69:7791–7799.
25. Wells SI, Francis DA, Karpova AY, Dowhanick JJ, Benson JD, Howley PM. Papillomavirus E2 induces senescence in HPV-positive cells via pRB- and p21(CIP)-dependent pathways. *Embo J.* 2000;19:5762–5771.
26. Steenbergen RD, Hermsen MA, Walboomers JM, et al. Integrated human papillomavirus type 16 and loss of heterozygosity at 11q22 and 18q21 in an oral carcinoma and its derivative cell line. *Cancer Res.* 1995;55: 5465–5471.
27. Ferris RL, Martinez I, Sirianni N, et al. Human papillomavirus-16 associated squamous cell carcinoma of the head and neck (SCCHN): a natural disease model provides insights into viral carcinogenesis. *Eur J Cancer.* 2005;41:807–815.
28. Taxman DJ, Livingstone LR, Zhang J, et al. Criteria for effective design, construction, and gene knockdown by shRNA vectors. *BMC Biotechnol.* 2006;6:7.
29. Seedorf K, Krammer G, Durst M, Suhai S, Rowekamp WG. Human papillomavirus type 16 DNA sequence. *Virology.* 1985;145:181–185.
30. Naviaux RK, Costanzi E, Haas M, Verma IM. The pCL vector system: rapid production of helper-free, high-titer, recombinant retroviruses. *J Virol.* 1996;70:5701–5705.
31. Livak KJ, Schmittgen TD. Analysis of relative gene expression data using real-time quantitative PCR and the 2(-delta delta C(T)) method. *Methods.* 2001;25:402–408.
32. Butz K, Shahabeddin L, Geisen C, Spitkovsky D, Ullmann A, Hoppe-Seyler F. Functional p53 protein in human papillomavirus-positive cancer cells. *Oncogene.* 1995;10:927–936.
33. Butz K, Ristriani T, Hengstermann A, Denk C, Scheffner M. Hoppe-Seyler F. siRNA targeting of the viral E6 oncogene efficiently kills human papillomavirus-positive cancer cells. *Oncogene.* 2003;22:5938–5945.

34. Horner SM, DeFilippis RA, Manuelidis L, DiMaio D. Repression of the human papillomavirus E6 gene initiates p53-dependent, telomerase-independent senescence and apoptosis in HeLa cervical carcinoma cells. *J Virol.* 2004;78:4063–4073.
35. Lee BY, Han JA, Im JS, et al. Senescence-associated beta-galactosidase is lysosomal beta-galactosidase. *Aging Cell.* 2006;5:187–195.
36. Dimri GP, Lee X, Basile G, et al. A biomarker that identifies senescent human cells in culture and in aging skin in vivo. *Proc Natl Acad Sci USA.* 1995;92:9363–9367.
37. Gillison ML, Shah KV. Human papillomavirus-associated head and neck squamous cell carcinoma: mounting evidence for an etiologic role for human papillomavirus in a subset of head and neck cancers. *Curr Opin Oncol.* 2001;13:183–188.
38. Weinberger PM, Yu Z, Haffty BG, et al. Molecular classification identifies a subset of human papillomavirus–associated oropharyngeal cancers with favorable prognosis. *J Clin Oncol.* 2006;24:736–747.
39. Haraf DJ, Nodzenski E, Brachman D, et al. Human papilloma virus and p53 in head and neck cancer: clinical correlates and survival. *Clin Cancer Res.* 1996;2:755–762.
40. van Houten VM, Snijders PJ, van den Brekel MW, et al. Biological evidence that human papillomaviruses are etiologically involved in a subgroup of head and neck squamous cell carcinomas. *Int J Cancer.* 2001; 93:232–235.
41. DeFilippis RA, Goodwin EC, Wu L, DiMaio D. Endogenous human papillomavirus *E6* and *E7* proteins differentially regulate proliferation, senescence, and apoptosis in HeLa cervical carcinoma cells. *J Virol.* 2003;77:1551–1563.
42. Gu W, Putral L, Hengst K, et al. Inhibition of cervical cancer cell growth in vitro and in vivo with lentiviral-vector delivered short hairpin RNA targeting human papillomavirus *E6* and *E7* oncogenes. *Cancer Gene Ther.* 2006;13:1023–1032.
43. Espinosa JM, Emerson BM. Transcriptional regulation by p53 through intrinsic DNA/chromatin binding and site-directed cofactor recruitment. *Mol Cell.* 2001;8:57–69.
44. Saramaki A, Banwell CM, Campbell MJ, Carlberg C. Regulation of the human p21(waf1/cip1) gene promoter via multiple binding sites for p53 and the vitamin D3 receptor. *Nucleic Acids Res.* 2006;34:543–554.
45. Owen-Schaub LB, Zhang W, Cusack JC, et al. Wild-type human p53 and a temperature-sensitive mutant induce Fas/APO-1 expression. *Mol Cell Biol.* 1995;15:3032–3040.
46. Muller M, Wilder S, Bannasch D, et al. p53 activates the CD95 (APO-1/Fas) gene in response to DNA damage by anticancer drugs. *J Exp Med.* 1998;188:2033–2045.
47. Bennett M, Macdonald K, Chan SW, Luzio JP, Simari R, Weissberg P. Cell surface trafficking of Fas: a rapid mechanism of p53-mediated apoptosis. *Science.* 1998;282:290–293.
48. Aguilar-Lemarroy A, Gariglio P, Whitaker NJ, et al. Restoration of p53 expression sensitizes human papillomavirus type 16 immortalized human keratinocytes to CD95-mediated apoptosis. *Oncogene.* 2002;21:165–175.
49. Carro MS, Spiga FM, Quarto M, et al. DEK expression is controlled by E2F and deregulated in diverse tumor types. *Cell Cycle.* 2006;5:1202–1207.
50. Lam EW, Bennett JD, Watson RJ. Cell-cycle regulation of human B-myb transcription. *Gene.* 1995;160:277–281.
51. Arsura M, Introna M, Passerini F, Mantovani A, Golay J. B-myb antisense oligonucleotides inhibit proliferation of human hematopoietic cell lines. *Blood.* 1992;79:2708–2716.
52. Wise-Draper TM, Allen HV, Jones EE, Habash KB, Matsuo H, Wells SI. Apoptosis inhibition by the human DEK oncoprotein involves interference with p53 functions. *Mol Cell Biol.* 2006;26:7506–7519.
53. Cervellera M, Raschella G, Santilli G, et al. Direct transactivation of the anti-apoptotic gene apolipoprotein J (clusterin) by B-MYB. *J Biol Chem.* 2000;275:21055–21060.
54. Grassilli E, Salomoni P, Perrotti D, Franceschi C, Calabretta B. Resistance to apoptosis in CTLL-2 cells overexpressing B-Myb is associated with B-Myb-dependent bcl-2 induction. *Cancer Res.* 1999;59:2451–2456.

Funding

Yale School of Medicine Institutional start-up funds (to A.P.); the Doris Duke Charitable Foundation (to P.W.); the Virginia Alden Wright Fund (to C.S.).

Notes

We thank Kristin Yates and Daniel DiMaio for advice and assistance. Portions of this study were presented at the 43rd Annual Meeting of the American Society of Clinical Oncology, June 2007. The study sponsors had no role in the design of the study; the collection, analysis, or interpretation of the data; the writing of the manuscript; or the decision to submit the manuscript for publication.

Present address: Department of Otolaryngology, Medical College of Georgia, Augusta, GA (P. Weinberger).

Manuscript received July 7, 2008; revised December 19, 2008; accepted January 13, 2009.